Can Casimir Forces be Asymmetric?

Robert L. DeBiase
203 Lindenwood Rd.
Staten Island, NY 10308
rldebiase@earthlink.net
(718) 948-9136

Abstract

There are two interpretations as to the source of energy behind the Casimir effect. In the first, the energy source is considered to be the zero-point fields in the vacuum of space between the plates.   In the second, the source is considered to come from the potential energy of atoms in the bulk matter making up the plates. It is believed that these two interpretations are equivalent.

The proximity force approximation (PFA), which can be premised upon the vacuum interpretation, is used to calculate forces between certain non-parallel plates. The PFA corrected for plasma wavelength and temperature has been used to gauge experiments, all of which have been done at room temperature until recently, with good agreement. When applied to, for example, sinusoidal half wavelength wedge geometry, anomalous asymmetric lateral forces appear. Because the PFA is premised upon tiny parallel plates, the local geometry of non-parallel plates is lost. When local geometry is considered, additional anomalous asymmetric forces can appear.

The pair-wise summation (PWS) approximation, based upon the bulk matter interpretation, does not produce asymmetric forces. Given the putative equivalence between the two interpretations, asymmetric PFA plate forces could be written off as artifact.

There are problems with the equivalence hypothesis, the most notable being that the PWS calculation is much smaller than the PFA, requiring a calibration factor and the two approximations produce forces in different directions for laterally asymmetric plates. The simplest way to reconcile the two points of view may be to abandon equivalence and instead consider the PWS bulk approximation a subset of the Proximity Force Approximation (PFA). The PFA would then represent the sum of vacuum and bulk components.

1. Introduction

As to the question whether the Casimir effect [1] can produce asymmetric forces with certain plate configurations , conventional wisdom says no. Asymmetric forces would imply that energy could be extracted from the quantum vacuum. Although Cole and Puthoff [4] have shown that extracting energy from the vacuum would not, in principle, violate the second law of thermodynamics, no one to date has shown a feasible extraction method.

It is true that Maclay and Forward proposed a gedanken spaceship powered by the dynamic Casimir effect where energy is pumped into a parallel plate cavity [11, 12], resulting in a propulsive force that was vanishingly small. However, no one, to the author's knowledge, has shown that a native Casimir force, using laterally asymmetric plates can produce an anomalous asymmetric force.

There are two interpretations as to the source of energy behind the Casimir effect [11, 12]. In the first, the energy source is considered to be the zero-point fields in the vacuum of space between and around the plates. Such a system could conceivably be open. The Proximity Force Approximation (PFA), also known as the Derjaguin approximation [5], can be premised upon an energy from the vacuum of space interpretation and can be used as a surrogate for that interpretation in calculations of laterally asymmetric plate geometries.

In the second interpretation, the source is considered to come from the potential energy of atoms in the bulk matter making up the plates, an extension of the Van der Waals forces. Without some other energy source input, such a system would be closed and could not produce anything other than equal and opposite forces between the plates, no matter their shape. The Pair Wise Summation (PWS) approximation can be used as a surrogate for the bulk interpretation in calculations of laterally asymmetric plate geometries.

The PFA and PWS calculations for lateral force will be compared and shown to be very different in both magnitude and direction of force in laterally asymmetric plate geometries. Even though it is believed that these two interpretations are equivalent [11, 12], it will be shown that another interpretation is that the energy from the PFA calculation is consistent with the sum of the energy from the bulk PWS calculation plus a purely vacuum energy component.

2. The Pair Wise Summation Approximation (PWS)

With the Pair Wise Summation approximation, the interaction energy potentials of pairs of polarizable atoms from two plates are added together as shown in Fig. 1.
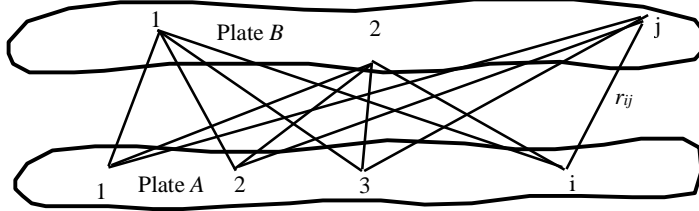

Fig. 1 – The summation of the energy potentials of pairs of atoms from the two plates

The energy potential of the atom pair *i, j* is described by the Casimir-Polder equation [7, 15]:

$$u(r_{ij}) = -\frac{\hbar c}{4\pi \cdot r_{ij}^7}\left[23 \cdot \left(\alpha_E^A \alpha_E^B + \alpha_M^A \alpha_M^B\right) - 7 \cdot \left(\alpha_E^A \alpha_M^B + \alpha_M^A \alpha_E^B\right)\right] \tag{1}$$

The parameter r_{ij} is the distance between atoms *i* and *j*, α_E and α_M are the electostatic and magnetic polarizability of the atoms respectively. Since $\alpha_M << \alpha_E$ in many cases, the Casimir Polder equation is sometimes simplified to [2]:

$$u(r_{ij}) = -\frac{\hbar c}{4\pi \cdot r_{ij}^7}\left[23 \cdot \alpha_E^A \alpha_E^B\right] \tag{2}$$

Since the forces on any pair of atoms are equal and opposite, the vector sums of all the forces for all the pairs of atoms will also be equal and opposite.

It will be noted that there is no restriction on the shape of the plates with PWS. Also, it is generally recognized that the total energy of the plates is not the sum of the energy from the individual pairs of atoms, but that further atoms in the plate are shielded by nearer atoms [15].

3. The Proximity Force Approximation (PFA)

The Proximity Force Approximation (PFA) is based upon the forces between two perfectly conducting parallel plates. The conducting plates suppress vibration modes of virtual photons between the plates but not outside the plates resulting in there being less energy inside the cavity than outside. The subsequent energy difference between outside and in results in an attractive force pushing the plates together.
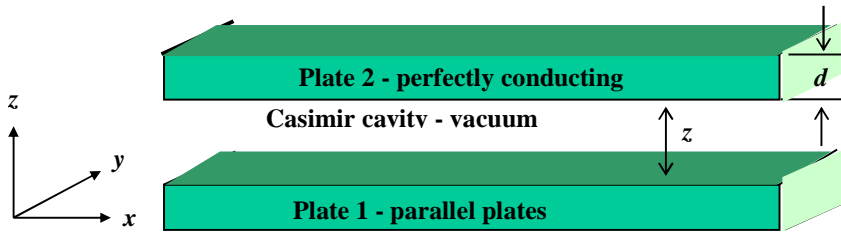

Fig. 2 – A Casimir cavity between two perfectly conducting parallel plates

The Casimir energy per unit *x, y* area e_{pp} derived from the zero point fields in a vacuum for two perfectly conducting parallel plates is:

$$e_{pp}(z) = -\frac{\hbar c \pi^2}{720 z^3} \tag{3}$$

where *z* is the distance between plates. The normal force per unit area on the plates is:

$$f(z) = -\frac{\partial e(z)}{\partial z} = -\frac{\partial}{\partial z}\left(-\frac{\hbar c \pi^2}{720 z^3}\right) = -\frac{\hbar c \pi^2}{240 z^4} \tag{4}$$

2

In a paper by Milonni, Cook and Goggin [13] the Casimir forces are calculated explicitly from the radiation pressure of the vacuum. The result for perfectly conducting parallel plates is the classical Casimir formulation of the force per unit area as given in Eq. 4.

3.1 – The proximity force approximation for non-parallel plates

Non-parallel plates can be thought of as multiple parallel plates as is shown in Fig. 3. For simplicity, the energy per unit area in the y direction is considered to be constant in this current consideration. But it does not need to be. The same methodology can be used to calculate forces between a sphere and flat plate, the result of which is the so called "Proximity Force Theorem", which states that the attracting force F_{sp} between a sphere of radius R separated from a flat plate by distance a is $2\pi R\, e_{pp}(a)$, where $e_{pp}(a)$ is the energy per unit area for two parallel flat plates separated by distance a [3, 9, 10].
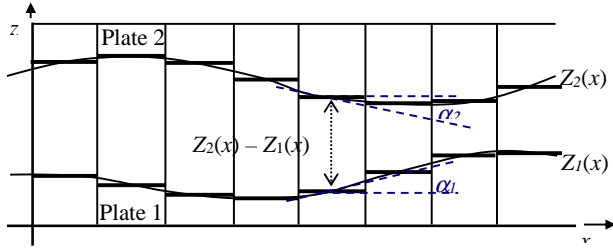

Fig. 3 – Dividing non-parallel plates into a set of parallel plates

The energy per unit x, y area e_{pp} can generally be easily determined for a general volumetric pixel given the geometry of the plates. From that the total plate energy can be determined by integrating over x, y area in terms of some geometric parameter for distance between plates - z_0.

To be clear, the normal direction is the direction between the plates, perpendicular to the parallel platelets - in the z direction. The lateral direction is along the plates in the x direction.

Given the energy e per unit x, y area at some location on the plate, forces per unit x, y area at that location can be determined in the following way:

$$\frac{d\vec{\mathbf{F}}}{dA_{xy}} = \vec{\mathbf{f}} = -\nabla e = -\frac{\partial e}{\partial x}\hat{\mathbf{i}} - \frac{\partial e}{\partial y}\hat{\mathbf{j}} - \frac{\partial e}{\partial z}\hat{\mathbf{k}} \tag{5}$$

Since energy per unit area is constant in the y direction for what is being considered in this paper, the middle force term in the direction of the **j** unit vector (the y direction) goes to zero. Also, while more "exact" methods [8, 14] exist for arbitrary geometries the geometries considered here are within the domain of the PFA.

3.2 – Calculation of normal forces

Using the right most term of Eq. 5 (the **k** unit vector term), the normal forces per unit x, y area for each plate can be calculated as follows, first for plate 1:

$$f_{z1} = -\frac{\partial e}{\partial z_1} = -\frac{\partial}{\partial z_1}\left(-\frac{\hbar c\pi^2}{720}\cdot\frac{1}{(z_2-z_1)^3}\right) = \frac{\hbar c\pi^2}{720}\cdot\left(\frac{-3\cdot(-1)}{(z_2-z_1)^4}\right) = \frac{\hbar c\pi^2}{240}\cdot\frac{1}{(Z_2-Z_1)^4} \tag{6}$$

Similarly for plate 2 the normal component of force per unit area will be:

$$f_{z2} = -\frac{\partial e}{\partial z_2} = -\frac{\partial}{\partial z_2}\left(-\frac{\hbar c\pi^2}{720}\cdot\frac{1}{(z_2-z_1)^3}\right) = \frac{\hbar c\pi^2}{720}\cdot\left(\frac{-3}{(z_2-z_1)^4}\right) = -\frac{\hbar c\pi^2}{240}\cdot\frac{1}{(Z_2-Z_1)^4} = -f_{z1} \tag{7}$$

Notice that f_{z1} on the bottom Z_1 plate is in the positive direction (up) and f_{z2} on the top Z_2 plate is in the negative direction (down). Thus the forces are attractive and since $f_{z1} = -f_{z2}$ for all parts of area A_{xy} the normal forces are equal and opposite for normal forces calculated using the PFA.

3

3.3 Calculation of lateral forces

As with the normal forces, the lateral forces per unit x, y area for each plate can be calculated as follows using **i** unit vector term of Eq. 5, first for plate 1:

$$f_{x1} = -\frac{\partial e}{\partial x_1} = -\frac{\partial}{\partial x_1}\left(-\frac{\hbar c \pi^2}{720}\cdot\frac{1}{\left(Z_2(x_2)-Z_1(x_1)\right)^3}\right) = \frac{\hbar c \pi^2}{720}\cdot\left(\frac{-3\cdot\left(-\frac{\partial Z_1(x_1)}{\partial x_1}\right)}{\left(Z_2(x_2)-Z_1(x_1)\right)^4}\right)$$

(8)

$$f_{x1} = \frac{\hbar c \pi^2}{240}\cdot\frac{\frac{\partial Z_1(x)}{\partial x}}{\left(Z_2(x)-Z_1(x)\right)^4}$$

Similarly for plate 2:

$$f_{x2} = -\frac{\partial e}{\partial x_2} = -\frac{\partial}{\partial x_2}\left(-\frac{\hbar c \pi^2}{720}\cdot\frac{1}{\left(Z_2(x_2)-Z_1(x_1)\right)^3}\right) = \frac{\hbar c \pi^2}{720}\cdot\left(\frac{-3\cdot\left(\frac{\partial Z_2(x_2)}{\partial x_2}\right)}{\left(Z_2(x_2)-Z_1(x_1)\right)^4}\right)$$

(9)

$$f_{x2} = -\frac{\hbar c \pi^2}{240}\cdot\frac{\frac{\partial Z_2(x)}{\partial x}}{\left(Z_2(x)-Z_1(x)\right)^4}$$

Total lateral forces on plates 1 and 2 may or may not be equal and opposite depending upon the asymmetric geometry of the plates. The reason, as can be seen in the equations for the two plates, the partial derivatives may not be equal.

3.4 Limitations of the PFA

Unlike pair wise summation, which can be used for plates of any shape, the PFA has restrictions on plate geometry.
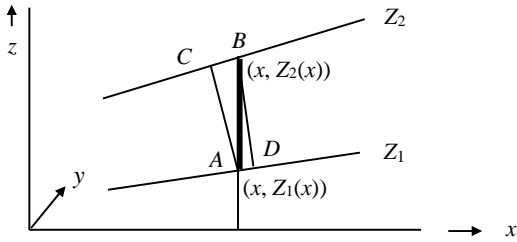

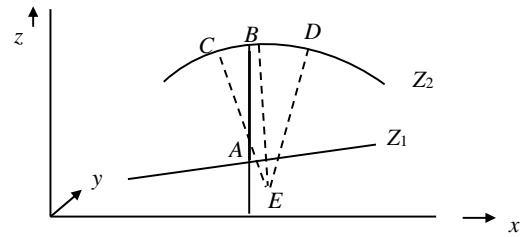Fig. 4a – Restrictions on plate slope   Fig. 4b – Restrictions on plate radius of curvature

In Fig. 4a, line AB is the distance used in the PFA as the distance between plates Z_1 and Z_2 at location x. Yet C on plate Z_2 is closer to A than B is, and D on plate Z_1 is closer to B than A is. Thus area at C would be expected to influence A greater than B does and D would influence B greater than A does, leading to the restriction that slopes on plates not be too great unless the distances between plates be far enough apart at these sections of plate as to contribute negligible influence (for example like a sphere and flat plate).

In Fig 4b, the center of curvature for a section of plate Z_2 is at E. If the curvature of Z_2 were any tighter or the distance between plates any larger, the center of curvature would fall within the cavity, leading to misleading estimation of the energy within the cavity. Thus there is a restriction that the center of curvature cannot fall within the cavity.

The restriction of Fig. 4a is the basis for a PFA extension [6] that could not only give a better estimate of forces between non-parallel plates but might also eliminate the lateral asymmetric force anomaly. However that is not what happens. The PFA extension not only maintains the lateral force asymmetry for laterally asymmetric plates but also produces an anomalous normal force asymmetry for normally asymmetric plates.

4. PFA Results for the Sinusoidal Half Wavelength Wedge

4.1 A mathematical model for a sinusoidally corrugated half wavelength wedge

The geometry of a sinusoidally corrugated half wavelength wedge is depicted in Fig. 5. The parameters used in the mathematical model based upon this geometry are contained in Table 1:

Parameter	Parameter Name	Value
L	Corrugation wavelength	1.2 μm*
A_1	Corrugation amplitude of plate 1	0.059 μm*
A_2	Corrugation amplitude of plate 2	Variable – between 0 and A_1
X_1	Phase displacement for plate 1	Set to 0
X_2	Phase displacement for plate 2	Variable
z_0	Parametric distance between plates	0.233 μm*
Y	Plate widths (plates 1 & 2)	1 cm

Table 1 – Parameters and values used in half wavelength wedge model

$$Z_2 = -A_2 \cdot \cos\left[\frac{2\pi}{L} \cdot (x - X_2)\right] + z_0$$

$$Z_1 = A_1 \cdot \cos\left(\frac{2\pi}{L} \cdot (x - X_1)\right)$$
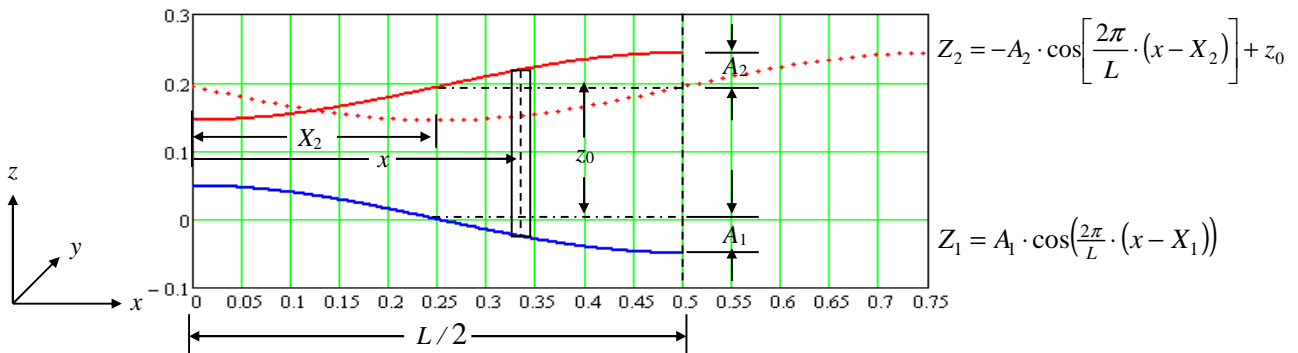
Fig. 5 – Geometry for half wavelength mathematical model

The parameter values in the table with asterisk were those used in the Chen, Mohideen, et. al. experiment of 2001 demonstrating the lateral Casimir force [3]. The *x* and z coordinates in Fig. 5 are in units of *L* the corrugation wavelength. The equations for Z_1 and Z_2 describe the *x, z* cross-section of plates 1 and 2 respectively.
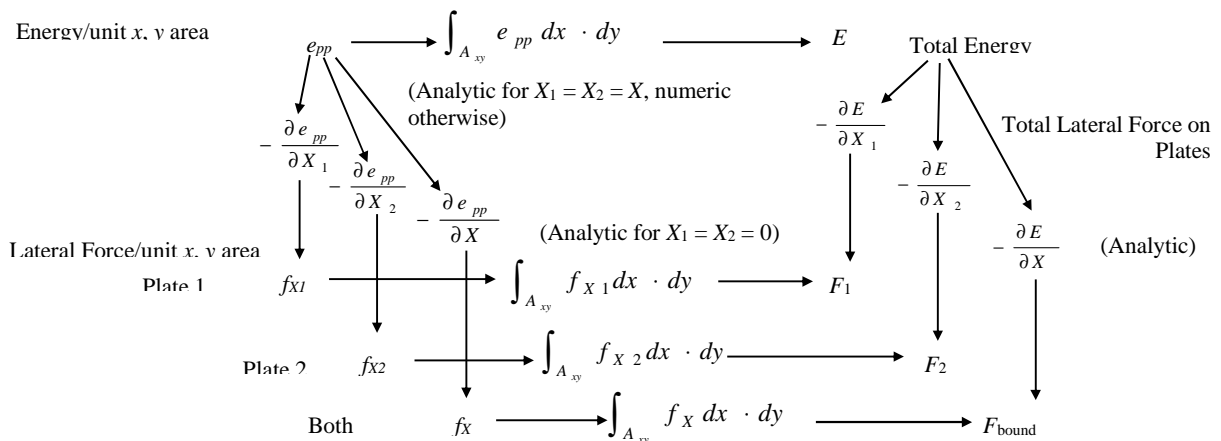
4.2 – Calculating total lateral forces on plates

Fig. 6 – Calculation flow for determining total force on plates 1 and 2 individually and collectively

As shown in Fig. 6, the process flow for calculating normal and lateral forces on plates begins with the energy per unit x, y area in terms of the parameters of the plate geometry. As might be expected, there are two ways to proceed. 1) Calculate the total energy first and then calculate the total force or 2) calculate the force per unit area first and then calculate the total force.

Total energy is calculated by integrating the energy per unit x, y area over the x, y area, which is the same for plates 1 and 2. The subsequent total energy can be used for calculating both normal and lateral forces. Lateral forces for use in the model are subsequently found by taking the partial derivative of the total energy with respect to the phase displacement X_2 for plate 2 and X_1 for plate 1. If $X_1 = X_2 = X$, the total force on both plates together can be found by taking the partial derivative of the total energy with respect to X.

The other way of proceeding is to calculate the lateral forces per unit x, y by taking the partial derivative of the energy per unit x, y area with respect to phase displacement X_2 for plate 2 and X_1 for plate 1. If $X_1 = X_2 = X$, the force per unit area on both plates together can be found by taking the partial derivative of the energy per unit area x, y with respect to X. Total lateral forces on plates 1 and 2 are then calculated by integrating the forces per unit x, y area over the x, y area. Note that the phase displacement variables X_1, X_2 and X are not the same as the area variable x.

4.3 – Calculating the angle of the lateral + normal force vector resultant

As one may have noticed, the lateral force per unit x, y area doesn't seem to have any physical meaning. So it is interesting to note the angle that the lateral plus normal force per unit x, y area vector resultant takes relative to the local area (not the x, y area).
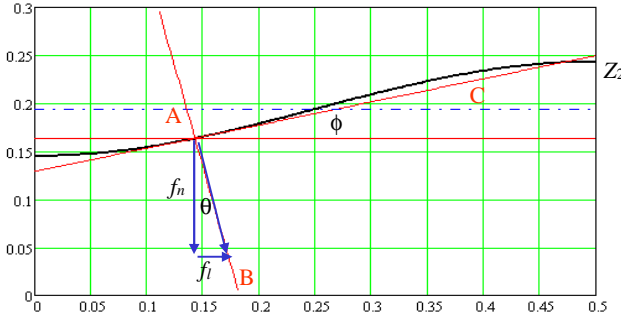

Fig. 7 – The angle of the lateral plus normal vector resultant relative to the local area

In Fig. 7, if the normal plus lateral vector resultant is perpendicular to the local area, then line AB will be perpendicular to the tangent to the curve AC and $\theta = \phi$.

First it is given that:

$$e_{pp} = -\frac{\pi^2 ch}{720(Z_2 - Z_1)^3}, \quad Z_1 = A_1 \cos\left(\frac{2\pi(x - X_1)}{L}\right) \quad \text{and} \quad Z_2 = z_0 - A_2 \cos\left(\frac{2\pi(x - X_2)}{L}\right)$$

The magnitude of the normal force per unit area for the Z_2 plate is then:

$$f_n = -\frac{\partial e_{pp}}{\partial Z_2} = -\frac{\pi^2 ch}{240(Z_2 - Z_1)^4} = -\frac{\pi^2 ch}{240\left(z_0 - A_2 \cos\left(\frac{2\pi(x - X_2)}{L}\right) - A_1 \cos\left(\frac{2\pi(x - X_1)}{L}\right)\right)^4} \tag{10}$$

While the magnitude of the lateral force per unit area for the Z_2 plate is:

$$f_l = -\frac{\partial e_{pp}}{\partial X_2} = \frac{\pi^3 ch A_2 \sin\left(\frac{2\pi(x - X_2)}{L}\right)}{120L\left(z_0 - A_2 \cos\left(\frac{2\pi(x - X_2)}{L}\right) - A_1 \cos\left(\frac{2\pi(x - X_1)}{L}\right)\right)^4} \tag{11}$$

Thus taking the absolute value Eq. 11 divided by Eq. 10:

$$\tan(\theta) = \left|\frac{f_l}{f_n}\right| = \frac{2\pi \cdot A_2 \sin\left(\frac{2\pi(x - X_2)}{L}\right)}{L}$$

More over, the derivative of Z_2 with respect to x is the slope of Z_2 at A and provides the means of determining ϕ. Thus:

$$\tan(\phi) = \frac{dZ_2}{dx} = \frac{2\pi \cdot A_2 \sin\left(\frac{2\pi(x-X_2)}{L}\right)}{L} = \tan(\theta) \qquad (12)$$

Thus, $\theta = \phi$ making the resultant force perpendicular to the local plate area, further making the resultant force per unit local plate area a PRESSURE. So while the lateral force per x, y area doesn't have physical meaning the vector sum of the lateral and normal forces per unit area does.

Similar arguments can be made in the case of the Z_1 plate.

This demonstration that force per unit plate area (not x, y area) is perpendicular to the plate area is consistent with the Milonni, Cook and Goggin [13] demonstration of radiation pressure for flat parallel plates and implies that non-parallel plates are also subject to radiation pressure.

4.4 Lateral Forces on Plates versus Varying Corrugation Phase X2

As a first test of the behavior of lateral forces on half wavelength wedge geometry depicted in Fig. 5, consider what happens when the corrugation phase X_2 of the Z_2 upper plate is changed while the bottom Z_1 plate remains stationary. Changing the corrugation phase of the upper plate is equivalent to imagining that the corrugations of the upper plate are extended in the positive and negative x directions. As X_2 increases, the upper corrugated plate moves from left to right. Only that part of the upper plate that is directly above the stationary lower plate participates in the Casimir effect as calculated by the PFA.

Starting with the energy per x, y area

$$e_{pp} = -\frac{\pi^2 c\hbar}{720\left(-A_2\cos\left(\frac{2\pi(x-X_2)}{L}\right) - A_1\cos\left(\frac{2\pi(x-X_1)}{L}\right) + z_0\right)^3} \qquad (13)$$

Calculate the lateral force per unit x, y area for plates 1 and 2 by taking the partial derivative of e_{pp} (Eq. 13) with respect to X_1 and X_2 respectively. After the derivatives are taken, set $X_1 = 0$ because plate 1 is stationary. The results for plate 1 are:

$$f_{X1}(X_2) = -\frac{\partial e_{pp}}{\partial X_1} = \frac{\pi^3 c\hbar \cdot A_1 \sin\left(\frac{2\pi}{L}x\right)}{120\left(-A_2\cos\left(\frac{2\pi}{L}(x-X_2)\right) - A_1\cos\left(\frac{2\pi}{L}x\right) + z_0\right)^4 L} \qquad (14)$$

Similarly, calculate the lateral force per unit x, y area for plate 2:

$$f_{X2}(X_2) = -\frac{\partial e_{pp}}{\partial X_2} = \frac{\pi^3 c\hbar \cdot A_2 \sin\left(\frac{2\pi}{L}(x-X_2)\right)}{120\left(-A_2\cos\left(\frac{2\pi}{L}(x-X_2)\right) - A_1\cos\left(\frac{2\pi}{L}x\right) + z_0\right)^4 L} \qquad (15)$$

The next step is to calculate the total lateral forces on each plate and the combination of plates together.

The total lateral force on plate 1 is found by integrating Eq. 14 by x and y:

$$F_1(X_2) = \int_{x=0}^{\frac{L}{2}} \int_{y=0}^{Y} f_{X1}(X_2)\,dy \cdot dx \quad \text{Repesented by} \quad \underline{\quad\quad} \quad \text{in Fig. 8} \qquad (16)$$

The total lateral force on plate 2 is found by integrating Eq. 15 by x and y:

$$F_2(X_2) = \int_{x=0}^{\frac{L}{2}} \int_{y=0}^{Y} f_{X2}(X_2)\,dy \cdot dx \quad \text{Represented by} \quad \underline{\quad\quad} \quad \text{in Fig. 8} \qquad (17)$$

The total lateral force from both plates is obtained by adding Eq. 16 and Eq. 17:

$$F(X_2) = F_1(X_2) + F_2(X_2) \qquad \text{Represented by} \quad \underline{\quad\quad} \quad \text{in Fig. 8} \qquad (18)$$
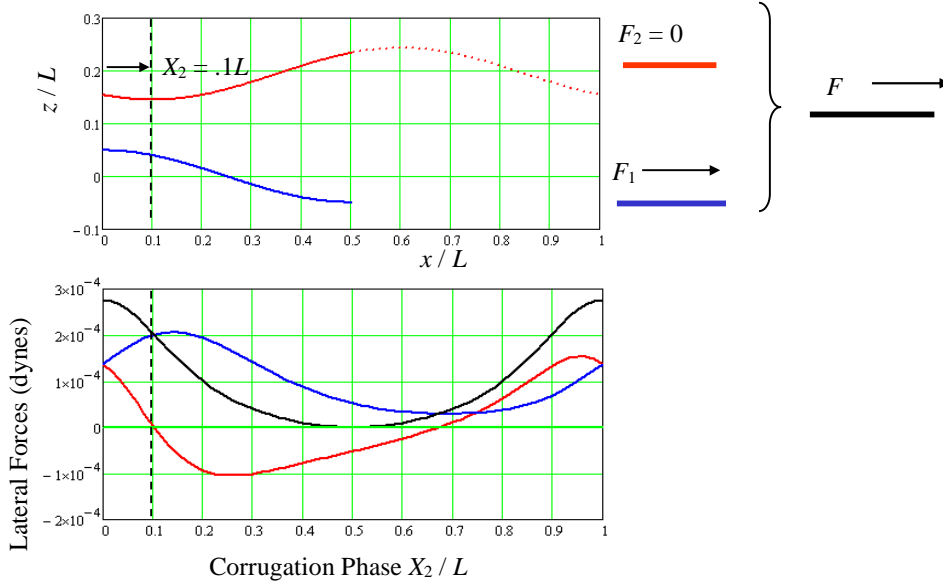
Fig. 8 – Lateral forces on plates

Observe that the forces on the top plate (in red) are sometimes positive (to the right) and sometimes negative (to the left). The forces on the stationary bottom plate (in blue) are always positive. The forces on the combination of plates (in black) are also always positive except for corruption phase $X_2 = L/2$ where it is 0.

4.5 Lateral Forces on Half Wave Plates with Parallel Plate "Wings" vs. X_2

The second test of lateral forces on half wavelength wedge plates involves extending the extremities of the sinusoidal wedges in both directions (for both plates) with parallel plate "wings". Again, the bottom plate will be held stationary and the top plate will be allowed to slide back and forth.

Starting with energy per unit x, y area:

$$e_{pp}(X_1, X_2) = -\frac{\hbar c \pi^2}{720} \cdot \frac{1}{\left(Z_2(X_2) - Z_1(X_1)\right)^3} \text{ where}$$

$$Z_1(X_1) = A_1 \cdot \cos\left(\frac{2\pi}{L} \cdot \min\left(\max(0, x - X_1), \frac{L}{2}\right)\right) \text{ and}$$

$$Z_2(X_2) = A_2 \cdot \cos\left(\frac{2\pi}{L} \cdot \min\left(\max(0, x - X_2), \frac{L}{2}\right) + \pi\right) + z_0 \tag{19}$$

Obtain the lateral force per unit x, y area for plate 1 by taking the partial derivative of e_{pp} (Eq. 19) by X_1:

$$f_{X1}(X_2) = -\frac{\partial e_{pp}(X_1, X_2)}{\partial X_1} = \frac{-\hbar c \pi^3 \cdot A_1}{120 L} \cdot \frac{\left(\frac{\partial}{\partial X_1} \min\left(\max(0, x - X_1), \frac{L}{2}\right)\right) \cdot \sin\left(\frac{2\pi}{L} \min\left(\max(0, x - X_1), \frac{L}{2}\right)\right)}{\left(Z_2(X_2) - Z(X_1)\right)^4} \tag{20}$$

Obtain the lateral force per unit x, y area for plate 2 by taking the partial derivative of e_{pp} (Eq. 19) by X_2:

$$f_{X2}(X_2) = -\frac{\partial e_{pp}(X_1, X_2)}{\partial X_2} = \frac{\hbar c \pi^3 \cdot A_2}{120 L} \cdot \frac{\left(\frac{\partial}{\partial X_2} \min\left(\max(0, x - X_2), \frac{L}{2}\right)\right) \cdot \sin\left(\frac{2\pi}{L} \min\left(\max(0, x - X_2), \frac{L}{2}\right) + \pi\right)}{\left(Z_2(X_2) - Z(X_1)\right)^4} \tag{21}$$

The total lateral force on Plate 1: $F_1(X_2)$ - can be obtained by integrating $f_{X1}(X_2)$, (Eq. 20) by x and y:

$$F_1(X_2) = \int_{x=0}^{1.5L} \int_{y=0}^{Y} f_{X1}(X_2) dy \cdot dx \quad \text{Represented by} \underline{\hspace{3cm}} \text{in Fig. 9} \tag{22}$$

The total lateral force on Plate 2: $F_2(X_2)$ - can be obtained by integrating $f_{X2}(X_2)$, (Eq. 21) by x and y:

8

$$F_2(X_2) = \int_{x=0}^{1.5L} \int_{y=0}^{Y} f_{X2}(X_2) dy \cdot dx \quad \text{Represented by} \quad \underline{\hspace{2cm}} \quad \text{in Fig. 9} \tag{23}$$

The total lateral force from both plates is obtained by adding Eq. 22 and Eq. 23:

$$F(X_2) = F_1(X_2) + F_2(X_2) \quad \text{Represented by} \quad \underline{\hspace{2cm}} \quad \text{in Fig. 9} \tag{24}$$
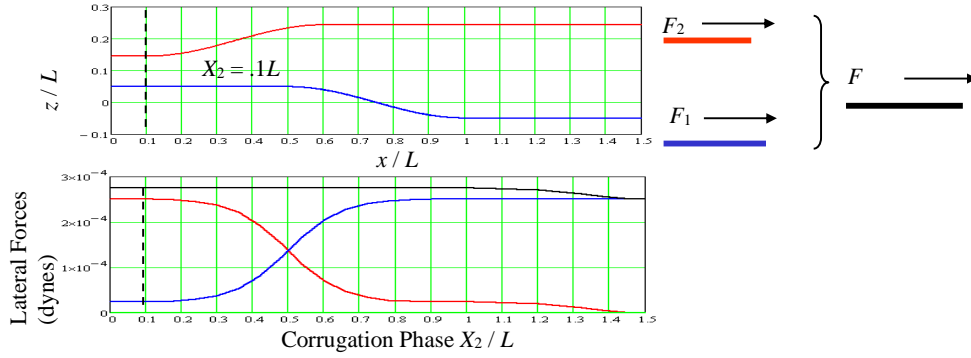

Fig. 9 – Lateral forces on half wave plates with parallel plate "wings" vs. X_2

4.5 Lateral forces on sliding half wave plates vs. X_2

The third test for the behavior of sinusoidally corrugated half wavelength wedge plates is similar to the first test except that the corrugations on the upper plate are not extended in the positive and negative *x* direction. Instead the only Casimir interaction according to the PFA is for those parts of the upper and lower plates that actually overlap each other.

Thus the energy per unit *x*, *y* area and the force per unit *x*, *y* area for plates 1 and 2 are the same as depicted in Eq. 13, 14 and 15 respectively.

The total force on plate 1:

For $X_2 > X_1 = 0$:   For $X_2 < X_1 = 0$:

$$F_1(X_2) = \int_{x=X_2}^{\frac{L}{2}} \int_{y=0}^{Y} f_{X1}(X_2) dy \cdot dx \qquad F_1(X_2) = \int_{x=0}^{X_2 + \frac{L}{2}} \int_{y=0}^{Y} f_{X1}(X_2) dy \cdot dx \tag{25}$$

The total force on plate 2:

For $X_2 > X_1 = 0$:   For $X_2 < X_1 = 0$:

$$F_2(X_2) = \int_{x=X_2}^{\frac{L}{2}} \int_{y=0}^{Y} f_{X2}(X_2) dy \cdot dx \qquad F_2(X_2) = \int_{x=0}^{X_2 + \frac{L}{2}} \int_{y=0}^{Y} f_{X2}(X_2) dy \cdot dx \tag{26}$$

The total force for both plates combined is: $F(X_2) = F_1(X_2) + F_2(X_2)$

For $X_2 > X_1 = 0$ $\underline{\hspace{2cm}}$ For $X_2 < X_1 = 0$ $\cdots\cdots\cdots$
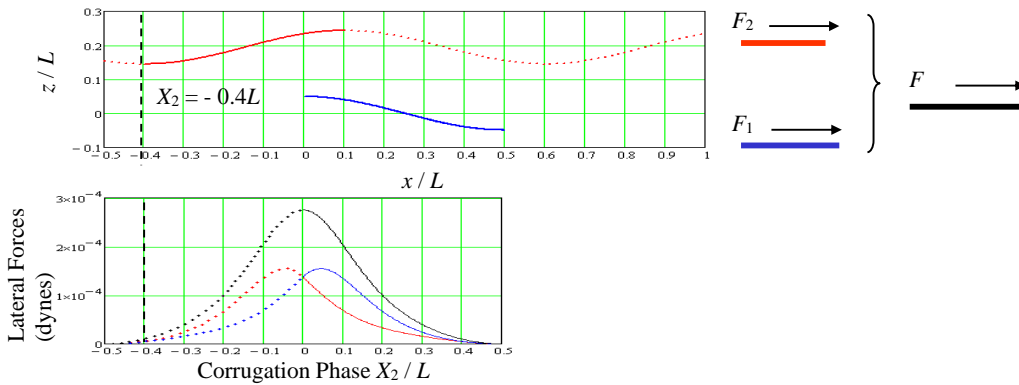

Fig. 10 – Lateral forces on sliding half wave plates vs. X_2

Thus all test 3 calculations for lateral forces on half wavelength wedges have shown asymmetric forces.

5. Differences between PWS and PFA

5.1 Calculating lateral forces on the sliding half wavelength wedge versus X_2 using PWS

In order to demonstrate the difference between the bulk and vacuum centric calculations, elements of the test 3 PFA calculation, the results of which are shown in Fig. 10, will be incorporated into a PWS calculation. For simplicity, the full PWS calculation will not be done but will instead be done for a few "atoms" representing the plates.

Representing the energy per pair of atoms in each of the plates is a simplified Casimir-Polder equation:

$$e_{PWS}(x_1, x_2, X_1, X_2) = -\frac{C}{\left((X_2 - X_1 + x_2 - x_1)^2 + (z_2(x_2) - z_1(x_1))^2\right)^{7/2}} \quad \text{where} \tag{27}$$

$z_1(x_1) = A_1 \cos\left(\frac{2\pi}{L} x_1\right)$, $z_2(x_2) = -A_2 \cos\left(\frac{2\pi}{L} x_2\right) + z_0$, $A_1 = A_2$ and C is an arbitrary constant.

The lateral forces per pair of atoms is then for plate 1:

$$f_{Lateral1}(x_1, x_2, X_1, X_2) = -\frac{\partial e_{PWS}(x_1, x_2, X_1, X_2)}{\partial X_1} = \frac{7C(X_2 - X_1 + x_3 - x_1)}{\left((z_2(x_2) - z_1(x_1))^2 + (X_2 - X_1 + x_3 - x_1)^3\right)^{9/2}} \tag{28}$$

For plate 2:

$$f_{Lateral2}(x_1, x_2, X_1, X_2) = -\frac{\partial e_{PWS}(x_1, x_2, X_1, X_2)}{\partial X_2} = \frac{-7C(X_2 - X_1 + x_3 - x_1)}{\left((z_2(x_2) - z_1(x_1))^2 + (X_2 - X_1 + x_3 - x_1)^3\right)^{9/2}} \tag{29}$$

The total lateral forces on each of the two plates is obtained by summing up the lateral forces on each of the pairs of atom for each plate.

Total lateral force on plate 1:

$$F_{Lateral1}(X_1, X_2) = \sum_{x_2=0}^{N} \sum_{x_1=0}^{M} f_{Lateral1}(x_1, x_2, X_1, X_2) \tag{30}$$

Total lateral force on plate 2:

$$F_{Lateral2}(X_1, X_2) = \sum_{x_2=0}^{N} \sum_{x_1=0}^{M} f_{Lateral2}(x_1, x_2, X_1, X_2) \tag{31}$$
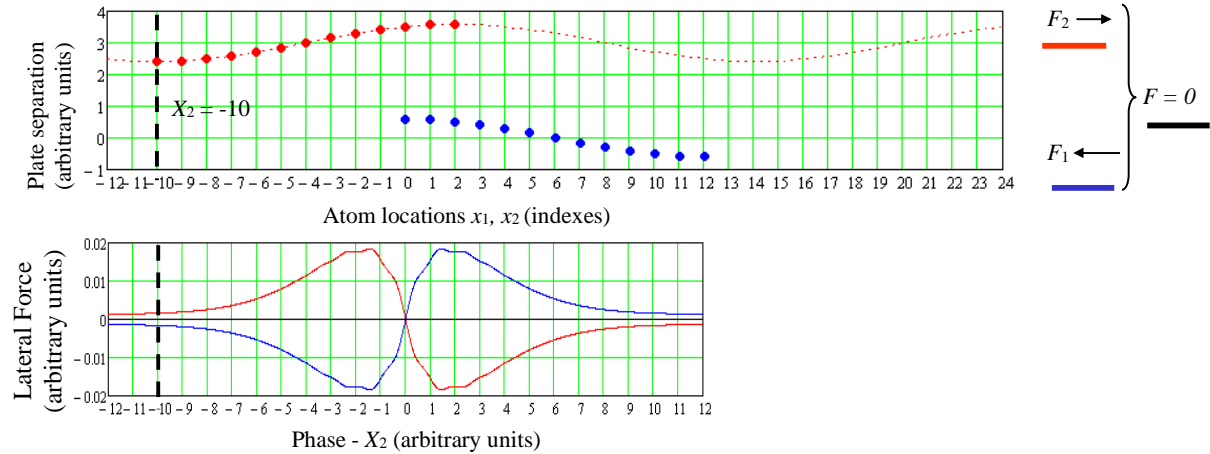

Fig. 11 - PWS Calculation for Half Wave Wedge Lateral Forces

It will be observed that lateral forces for the half wavelength wedge calculated by PWS cancel out whereas those calculated by PFA do not.

5.2 Deriving PWS equation for parallel plates

Doing a full PWS calculation for corrugated plates was dismissed in favor of a representative calculation involving a few "atoms". However a full calculation can be done for parallel plates and then compared with the vacuum oriented calculation. Fig. 12 shows a diagram defining the parameters for the PWS calculation of two parallel flat plates.
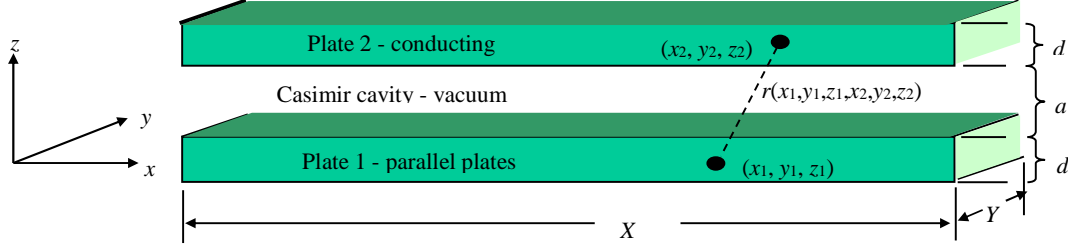

Fig. 12 – Diagram for deriving PWS equation for parallel plates

The interaction energy between a pair of atoms in Plates 1 and 2 can be found from the simplified Casimir-Polder equation first shown in Eq. 2 and here repeated with some modifications:

$$u\left(r\left(x_1, y_1, z_1, x_2, y_2, z_2\right)\right) = -\frac{23\hbar c \cdot \alpha_{E1}\alpha_{E2}}{4\pi \cdot r\left(x_1, y_1, z_1, x_2, y_2, z_2\right)^7} \quad \text{where}$$

$r\left(x_1, y_1, z_1, x_2, y_2, z_2\right) = \sqrt{\left(x_2 - x_1\right)^2 + \left(y_2 - y_1\right)^2 + \left(z_2 - z_1\right)^2}$ and a_{E1}, a_{E2} = electrostatic polarizability of atoms. *(32)*

The total energy between plates is found by integrating over the volumes of both plates:

$$U\left(a,d\right) = -\frac{23\hbar c \cdot \alpha_{E1}\alpha_{E2} \cdot \eta^2}{4\pi} \int_{z_1=0}^{d} \int_{z_2=d+a}^{2d+a} \int_{y_1=0}^{Y} \int_{y_2=0}^{Y} \int_{x_1=0}^{X} \int_{x_2=0}^{X} \frac{dx_2 \cdot dx_1 \cdot dy_2 \cdot dy_1 \cdot dz_2 \cdot dz_1}{r\left(x_1, y_1, z_1, x_2, y_2, z_2\right)^7}$$

where η = number of atoms per unit volume. *(33)*

After much calculation the normal force on plate 2 becomes:

$$F_z\left(a,d\right) = -\frac{\partial U\left(a,d\right)}{\partial a} = -\frac{23\hbar c \cdot \alpha_{E1}\alpha_{E2} \cdot \eta^2}{4\pi} \cdot \frac{\pi}{10} \cdot XY \cdot \left(\frac{1}{a^4} - \frac{2}{\left(a+d\right)^4} + \frac{1}{\left(a+2d\right)^4}\right) + SmallerTerms$$ *(34)*

When $d = 0$, $F_z = 0$, which makes sense because when $d = 0$ there are no plates and thus no force between plates. When d is much greater than a, but much less than X or Y, F_z becomes like the vacuum centric Casimir equation because the terms with d in them go to zero. For X approximately equal to Y and plate separation a less than $X / 1000$, *SmallerTerms* is approximately less than one part in a thousand.

5.3 Comparing the PWS with the vacuum centric solution for parallel plates

First a comparison of constants used in both calculations:

Universal		Bulk (PWS)	Vacuum (PFA)
$\hbar$	Reduced Planck's constant	1.055 x 10⁻²⁷ erg*s	1.055 x 10⁻²⁷ erg*s
c	Speed of light	2.998 x 10¹⁰ cm/s	2.998 x 10¹⁰ cm/s
Material Specific			
α_E	Electrostatic polarizability of atom	1.88 x 10⁻²⁴ cm³/atom (gold)	N / A
η	Number of atoms per unit volume	5.9 x 10²² atoms/cm³ (gold)	N / A

Table 2 – Constants used in calculation of Casimir forces

For d much greater than a, $F_{PWS} = -\dfrac{23\hbar c \alpha_E{}^2 \eta^2 \cdot XY}{40a^4}$ and $F_{pp} = -\dfrac{\hbar c \pi^2 XY}{240a^4}$,

Resulting in the ratio: $\dfrac{F_{PWS}}{F_{pp}} = \dfrac{138\alpha_E{}^2 \eta^2}{\pi^2} = 0.172$ for gold. *(35)*

The conclusion is that F_{PWS} is much less than F_{pp}, which leads to the question: If bulk and vacuum models are equivalent, Why is the ratio not closer to 1?

Proceeding a step further, it is interesting to determine the dependency of the force ratio in Eq. 35 on plate thickness d.

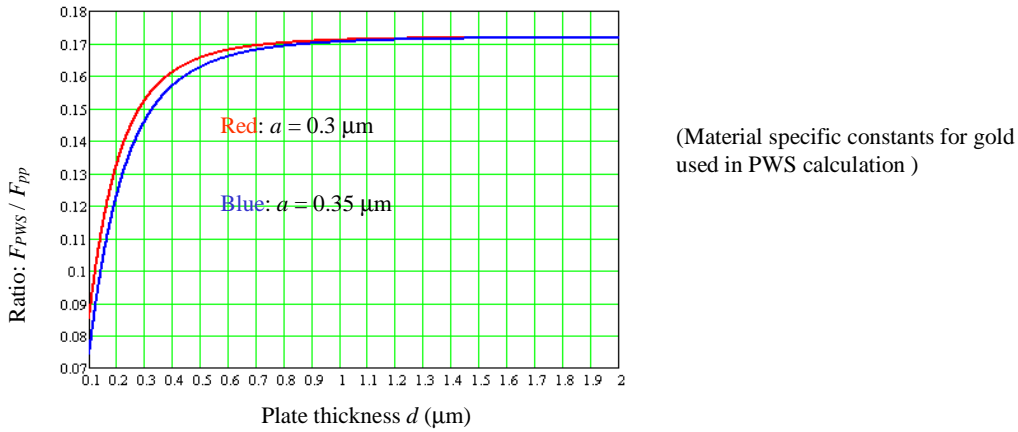(Material specific constants for gold used in PWS calculation)

Fig. 13 – Dependency of force ratio F_{PWS} / F_{pp} on plate thickness d

It is known that nearer atoms shield further atoms, so some effective distance needs to be used in PWS calculations resulting in the force ratio $F_{PWS} / F_{pp} < 0.172$.

Differences between the bulk and vacuum calculations can be summarized as follows:
• Laterally asymmetric geometries result in laterally asymmetric forces for PFA
• If bulk & vacuum models are equivalent, Why is F_{PWS} / F_{pp} ratio for parallel plates not closer to 1?
• Screening of distant atoms by closer atoms should make difference greater
• Lateral forces calculated by PWS cancel out. Those calculated by PFA do not.

6. Are bulk and vacuum models complementary?

The general consensus is that the bulk and vacuum interpretations of the Casimir effect are equivalent. In view of the differences seen from calculations using the PWS and the PFA, could the two interpretations be complementary instead of equivalent?

There are two ways the bulk and vacuum models could be complimentary:

1. By making the total energy the sum of E_{PFA} and E_{PWS}. However, this approach requires a new correction or corrections to make it work and the parameters needed in the new correction don't make sense.

2. By making the total energy E_{PFA} and the vacuum portion $E_{PFA} - E_{PWS}$. With this approach forces from the bulk (PWS) model cancel out.

The second method is the preferred way to make bulk (PWS) and vacuum models complimentary.

For the case of normal forces and the PFA, the normal forces are already equal and opposite. PWS also produces equal and opposite forces, so differences in the magnitude of normal forces are trivially zero. However, for the extended PFA asymmetric normal forces are possible.

$$F_{Vacuum2} \quad - \quad F_{Vacuum1} \quad =$$
$$(F_{extPFA2} - F_{PWS}) - (F_{extPFA1} - F_{PWS}) \quad =$$
$$F_{extPFA2} \quad - \quad F_{extPFA1} \quad = \Delta F_{extPFA}$$
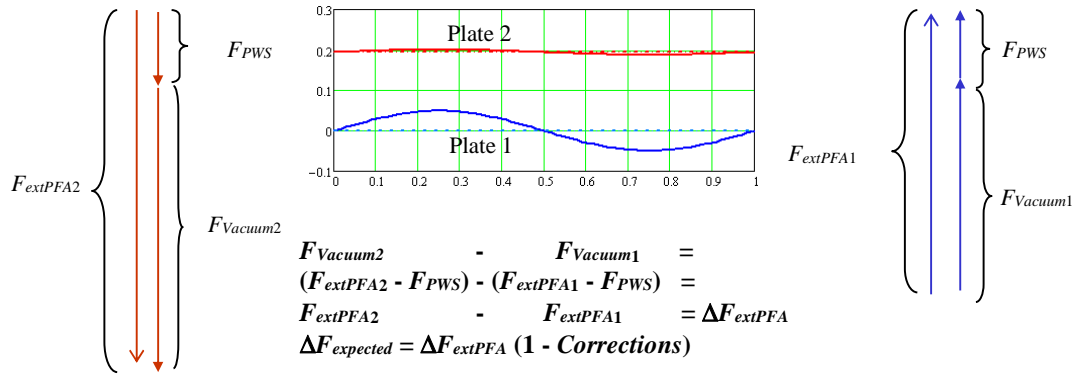$$\Delta F_{expected} = \Delta F_{extPFA} \, (1 - Corrections)$$

Fig. 14a – Complementary normal forces with extended PFA

As can be seen in Fig. 14a, all asymmetry is coming from the vacuum portion.

In the case of lateral forces the PFA allows asymmetric forces, PWS does not. Fig. 14b shows how the PFA and PWS forces could be complementary when the PFA is the sum of PWS and a purely vacuum component.
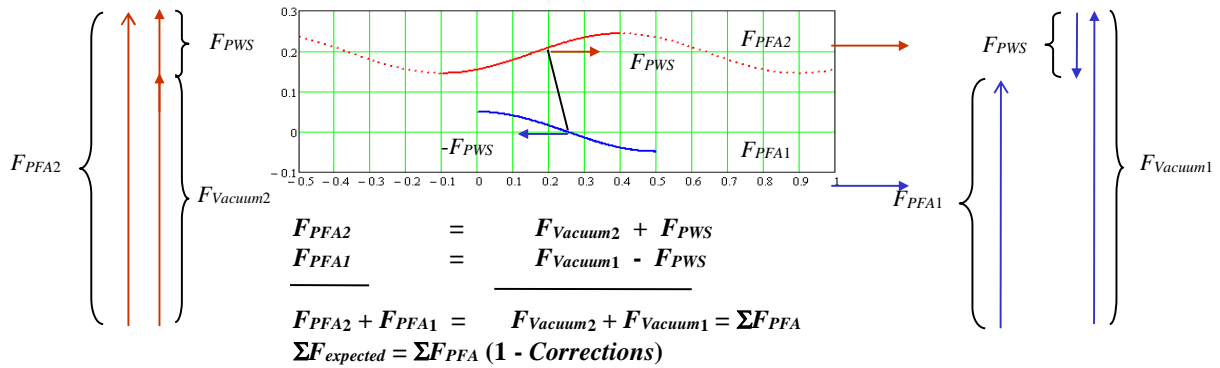

$$F_{PFA2} \quad = \quad F_{Vacuum2} + F_{PWS}$$
$$F_{PFA1} \quad = \quad F_{Vacuum1} - F_{PWS}$$

$$F_{PFA2} + F_{PFA1} \; = \quad F_{Vacuum2} + F_{Vacuum1} = \Sigma F_{PFA}$$
$$\Sigma F_{expected} = \Sigma F_{PFA} \, (1 - Corrections)$$

Fig. 14b – Complementary lateral forces with PFA

As can be seen in Fig. 14b, all asymmetric forces are coming from the vacuum portion of the PFA.

7. Conceptual experiments testing asymmetric forces

7.1 – The typical experiment done today

Typically, experiments are set up to measure forces on one plate or the other, but not both plates at the same time. In most cases one plate is a sphere and the other a flat plate. Two flat plates are generally not used because of the great difficulty at maintaining parallelism at the requisite accuracy. There is no issue of parallelism when one plate has a spherical surface [10].
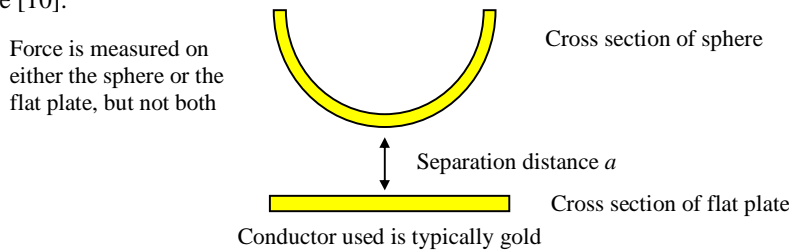

Fig. 15 - A typical experimental setup

Experiments that have been done to date implicitly assume the Casimir forces are equal and opposite. They are not capable of measuring asymmetric forces.

13

7.2 – A test of the PFA prediction of asymmetric lateral forces for sinusoidal half wavelength wedge

In order to measure asymmetric forces, both plates must be constrained so as to not move relative to one another as depicted in Fig. 16. Parallel plate "wings" have been added on to the half sine wave components on each plate. As shown in Fig. 9, the "wings" make the experimental apparatus less sensitive to lateral positioning of the top plate over the bottom.

The parameters in the diagram and their suggested values are as follows:

L^* = Corrugation wavelength: 1.2 μm, A^* = Corrugation amplitude: .059 μm, $z_0{}^*$ = Parametric distance between plates: 0.233 μm and Y = Plate widths: 1 cm. The values of the dimensions with asterisk are those used in the Chen, Mohideen experiment.
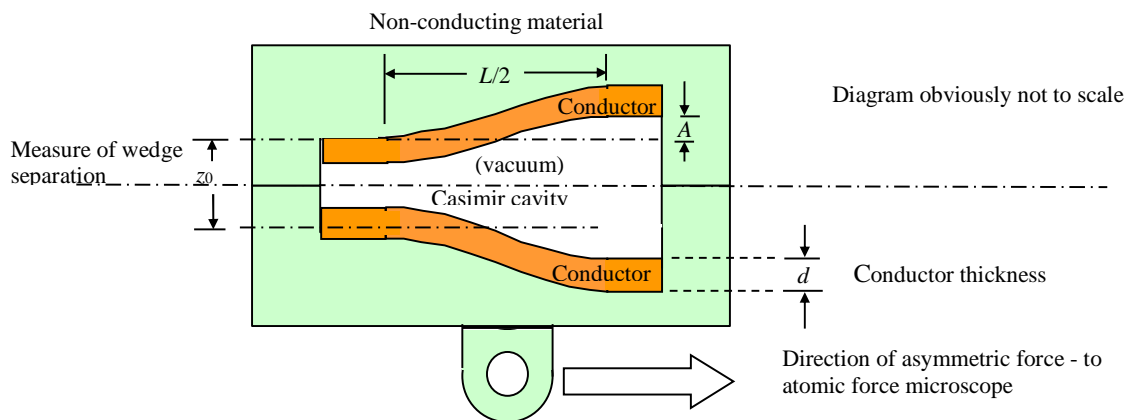

Fig. 16 - Testing PFA prediction of asymmetric lateral forces for sinusoidal half wavelength wedge

For a single half wavelength times 1 cm width, there is an expected lateral force about 2 to 3 x 10^{-4} dynes. If it were to be assumed that the cavity depicted in Fig. 16 were to be repeated multiple times – about 5,000 times in a 1 cm length plate – it might be possible to expect from 1 to 1.5 dynes for the entire system. Such a system would not need an atomic force microscope to measure the forces.

8. Conclusions and implications

8.1 Conclusions

Conclusions are summarized in Table 3. The extended PFA is herein included, even though it was just cursorily mentioned, for completeness.

Characteristics	PFA	Extended PFA	PWS
Premised On	Vacuum fields	Vacuum fields	Bulk matter
Asymmetric normal forces	No	Yes	No
Asymmetric lateral forces	Yes	Yes	No
Force/unit area consistent with radiation pressure?	Yes	Not tested	Not applicable
Becomes classical case for parallel plates	Yes	Yes	No - requires normalization or calibration
Bulk & vacuum views complementary?	PFA & Extended PFA are vector sums of vacuum and bulk (PWS) components		

Table 3 – Summary of conclusions from consideration of PFA predictions of lateral asymmetric forces for half wavelength wedge

8.2 Scientific implications

- Scientific calculations showing equivalence of bulk and vacuum models have not been done for non-parallel plates (to author's best reckoning). Assertion of equivalence is based upon belief.

- Experiments to detect asymmetric forces have not been performed (also to the author's best reckoning).

- Detection of asymmetric forces would disprove equivalence between vacuum and bulk views of Casimir effect. Non-detection would not prove the converse however.

- Detection of asymmetric macroscopic forces would send scientists back to the drawing board regarding expansion of the universe and why such expansion has not ripped the universe apart.
- If asymmetric forces are detected, they could provide a new probe into quantum vacuum.
- Caveat - calculations shown were engineering not scientific calculations. However the engineering surrogate (PFA) CLEARLY shows asymmetric lateral forces result for the laterally asymmetric half wavelength wedge. The PFA is still being used to gauge experiments and the parameters used were those used in a classic experiment.

8.3 Technological implications

The best way to assess the technological implications of the putative asymmetric forces predicted by the PFA for half wavelength wedges is to do a back of the envelope calculation for the force that could be produced from a 1 cm X 1 cm X 1cm volume making appropriate assumptions. Conservatively assume for example that there are between 5,000 and 10,000 cavities per 1 cm length and 10,000 layers per 1 cm height. Further assume that the 1 cm^3 volume has a density approximately that of water and each cavity of one half wavelength times 1 cm width produces a force of 2 x 10^{-4} dynes to 3 x 10^{-4} dynes. Then the cubic centimeter cube would produce the following:

Lateral force / cm^3 = between 10,000 dynes / cm^3 and 30,000 dynes/cm^3

Intrinsic acceleration = (Lateral force / cm^3) / (density = 1 g / cm^3) = between 10 g_E and 30 g_E

Implied Mass Fractions: 1 part propulsion mass to 5 to 19 parts vehicle and payload mass

Such mass fractions are more like that of an airplane than a rocket. Moreover the constant accelerations simultaneously solve the problems of weightlessness for astronauts and long interplanetary travel times with implicit radiation exposure. Intrinsic accelerations on the high end would make possible the first practical flying car.

Of course all of these implications depend upon the PFA predictions being real.

It has been shown that the proximity force approximation predicts anomalous asymmetric lateral forces for asymmetric lateral geometries and that the forces per unit plate area calculated with the proximity force approximation are consistent with a radiation pressure. Further, it has been plausibly shown that the bulk and vacuum models can co-exist if they are complementary instead of equivalent.

It has not been shown that Casimir plates with asymmetric lateral geometries actually produce asymmetric forces. The predicted asymmetric forces may be a result of an artifact of the proximity force approximation itself. And, it still might be true that the bulk and vacuum models are equivalent.

Non-the-less the proximity force approximation predictions should stimulate curiosity to examine the possibility of asymmetric forces in more detail.

References

[1] Casimir H.B.G. "On the attraction between two perfectly conducting plates," *Proc. K. Ned. Akad. Wet.* 1948; **51**: 793-795.

[2] Casimir H.B.G. and Polder D., "The Influence of Retardation on the London-van der Waals Forces," *Physical Review* 1948; **73(4)**.

[3] Chen E., Mohideen U., Klimchitskaya G.L., Mostepanenko V.M. "Demonstration of the lateral Casimir force," *PhysRevLett* 2002; **88(10)**: 101801.

[4] Cole D. C. and Puthoff H. E., "Extracting energy and heat from the vacuum," *Phys Rev E*; 1993, **48**: 1562-1565.

[5] Dalvit DAR, Neto PAM, Lambrecht A, Reynaud S. "Lateral Casimir–Polder force with corrugated surfaces," *J. Phys. A: Math. Theor.* 2008; **41**: 164028 (11pp).

[6] DeBiase R.L. "Are Casimir forces conservative," *Space, Propulsion & Energy Sciences International Forum* – 2012, available online at www.sciencedirect.com.

[7] Kenneth O., Klich I., Mann A., Revzen M., "Repulsive Casimir Forces," *Physical Review Letters* 2002; **89**(3), 033001

[8] Milton K.A., Wagner J. "Multiple scattering methods in Casimir calculations," *J. Phys. A: Math. Theor.* 2008; **41**: 155402.

[9] Lambrecht A., Neto P.A.M., Reynaud S. "The Casimir effect within scattering theory," *New Journal of Physics* 2006; **8**: 243.

[10] Lamoreaux S.K. "Demonstration of the Casimir force in the 0.6 to 6   m range," *PhysRevLett* 1997; **78(1)**: 5-8.

[11] Maclay G.J., Forward R.L. "A gedanken spacecraft that operates using the quantum vacuum (dynamic Casimir effect)," *Foundations of Physics* 2004; **34(3)**: 477-500.

[12] Maclay G.J., "Thrusting against the quantum vacuum," In: Millis MG, Davis EW, editors, *Frontiers of Propulsion Science*, In: Lu FK, editor, *Progress in Astronautics and Aeronautics*, Reston, Va.: AIAA; 2008, **227:** p. 391-422.

[13] Milonni P.W., Cook RJ, Goggin ME. "Radiation pressure from the vacuum: Physical interpretation of the Casimir force," *Phys Rev A.* 1988; **38**: 1621-3.

[14] Rodriguez A., Ibanescu M., Iannuzzi D., Capasso F., Joannopoulos J.D., Johnson S.G. "Computation and Visualization of Casimir Forces in Arbitrary Geometries," *PhysRevLett* 2007; **99**: 080401.

[15] Tajmar M, "Finite Element Simulation of Casimir Forces in Arbitrary Geometries," *Int. J. Mod. Phys. C* 2004; **15**: 1387-1395.